Finite Element Analysis of Mixed Convection Heat Transfer through a Vertical Wavy Isothermal Channel

H.Shokouhmand, S.M.A.Noori Rahim Abadi

Abstract— In this paper, mixed convection heat transfer through a vertical wavy isothermal channel is investigated numerically. In present study, the hot sinusoidal vertical walls are at constant temperature and the cold flow enters the channel at the bottom side. The numerical model is based on a 2D Navier-Stokes incompressible flow and energy equation solver on unstructured grid. The governing equations consist of continuity, momentum and energy equations are solved numerically by finite element method using Characteristic Based Split (CBS) algorithm. The effect of Reynolds, Prandtl and Grashof numbers on flow and thermal fields are investigated. The variations of local Nusselt number along the vertical walls are also presented.

Keywords— Mixed Convection, Finite Element Method, Wavy Channel.

I. Introduction

Mixed convection involves features from both forced and natural flow conditions. In mixed convection flows, the forced convection and free convection effects are comparable in magnitudes. Thus, mixed convection occurs if the effect of buoyancy forces on a forced flow or the effect of forced flow on a buoyant flow is significant. The governing non-dimensional parameters for the description of mixed convection flows are Grashof number (Gr), Reynolds number (Re) and Prandtl number (Pr). The ratio Gr/Re^2 is also named Richardson number (Ri) that indicate the strength of the natural and forced convection flow effects The limiting case $Ri\rightarrow 0$ and $Ri\rightarrow\infty$ correspond to the forced and natural convection flows, respectively.

It is necessary to study the heat and mass transfer from an irregular surface because irregular surfaces are often present in many applications such as micro-electronic devices, flat-plate solar collectors and flat-plate condensers in refrigerators [1], and geophysical applications (e.g., flows in the earth's crust [2]), underground cable systems, electric machinery, cooling system of micro-electronic devices, etc. In addition, roughened surfaces could be used in the cooling of electrical and nuclear components where the wall heat flux is known. One of the reasons why a roughened surface is more efficient in heat transfer is its capability to promote fluid motion near the surface; in this way a complex wavy surface, a sum of two or more sinusoidal surfaces, is expected to promote a larger heat-transfer rate than a single sinusoidal surface. This complex geometry will promote a correspondingly complicated motion in the fluid near the surface; this motion is described by the nonlinear boundary-layer equations. This expectation is the basis of the current study even though only laminar mixed convection is studied. A vast amount of literature about convection along a sinusoidal wavy surface is available for different heating conditions and various kinds of fluids [3–7]. Recently Ashjaee et al. [8] have investigated the problem of free convection along a vertical wavy surface experimentally and numerically. The investigation was carried out for three different amplitude–wavelength ratios and Rayleigh number based on the length of the wavy surface ranging from $2.9*10^5$ to $5.8*10^5$. Results indicate that the frequency of the local heat transfer rate is the same as that of the wavy surface and the average heat transfer coefficient decreases as the as the amplitude- wavelength ratio increases. The natural convection heat transfer from an isothermal vertical wavy surface was first studied by Yao [9–11] and using an extended Prantdl's transposition theorem and a finite-difference scheme. He proposed a simple transformation to study the natural convection heat transfer from isothermal vertical wavy surfaces, such as sinusoidal surface. Chiu and Chou [12] studied the natural convection heat transfer along a vertical wavy surface in micropolar fluids. Chen and Wang [13,14] analyzed transient forced and free convection along a wavy surface in microfluids. Cheng [15,16] has investigated coupled heat and mass transfer by natural convection flow along a wavy conical surface and vertical wavy surface in a porous medium.

The aim of this study is to investigate the effects of parameters such as Grashof number, Reynolds number and Prandtl number on flow and thermal fields through the channel. The local Nusselt number of vertical walls along the channel at the wide range of governing parameters (Re, Pr, Gr numbers) are presented. The governing equations including continuity, Navier–Stokes and energy equations are solved numerically by Galerkin finite element method based on the characteristic based split (CBS) algorithm.

II. Governing Equations

A two-dimensional vertical wavy channel and related dimensionless boundary conditions are illustrated in Fig. 1. The shapes of the side wavy surfaces profile are as the following pattern:

$$x=\frac{D}{2}\pm A\sin(2\pi yk) \tag{1}$$

H.Shokouhmand is professor of the School *of Mechanical Engineering, College of Engineering, University of Tehran, Tehran, Iran* (e-mail: hshokoh@ ut.ac.ir).

S.M.A.Noori is M.S student of the School *of Mechanical Engineering, College of Engineering, University of Tehran, Tehran, Iran* (corresponding author to provide phone: 00982614403646; e-mail: a.noori1364@ gmail.com).

Where A is the dimensionless amplitude of the wavy surfaces and k is the number of undulation (z=5). D and L (L=6D) are the mean diameter and the length of the channel, respectively. The cold fluid enters the channel with the conditions, $T=T_c$, $u=U_0$ and v=0. The sinusoidal vertical walls of the channel are at constant temperature $T=T_h$. The flow is assumed to be laminar and the fluid is assumed to be incompressible, with constant physical properties except for the density variation which is taken into account through the Boussinesq approximation. Also viscous dissipation and pressure work are considered negligible.

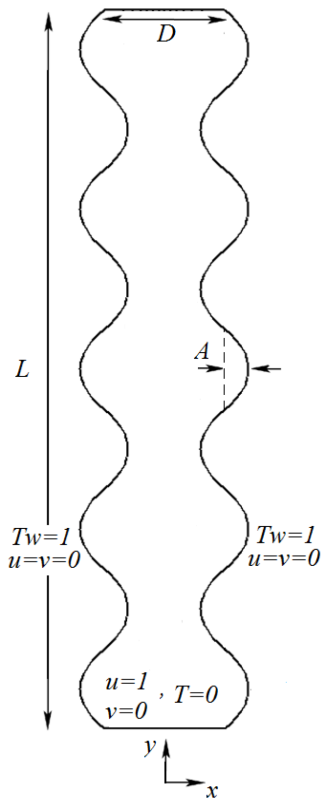

Fig1, physical model

Based upon the characteristics scales of D, U_0, T_h and T_c, the dimensionless variables are defined as follows:

$$x^* = \frac{x}{D} \quad y^* = \frac{y}{D} \quad u^* = \frac{u}{U_0} \quad v^* = \frac{v}{U_0}$$

$$p^* = \frac{p}{\rho U_0^{\ 2}} \quad T^* = \frac{T - T_c}{T_h - T_c}$$

$$Gr = \frac{gBD^3(T_h - T_c)}{\nu^2} \quad \Pr = \frac{\nu}{\alpha} \quad \mathrm{Re} = \frac{U_0 D}{\nu} \tag{2}$$

Therefore the non-dimensional governing equations are (the stars were omitted for simplicity):

Continuity equation:

$$\frac{\partial u}{\partial x} + \frac{\partial v}{\partial y} = 0 \tag{3}$$

U momentum equation:

$$\frac{\partial u}{\partial t} + u\frac{\partial u}{\partial x} + v\frac{\partial u}{\partial y} = -\frac{\partial p}{\partial x} + \frac{1}{\mathrm{Re}}\left(\frac{\partial^2 u}{\partial^2 x} + \frac{\partial^2 u}{\partial^2 y}\right) \tag{4}$$

V momentum equation:

$$\frac{\partial v}{\partial t} + u\frac{\partial v}{\partial x} + v\frac{\partial v}{\partial y} = -\frac{\partial p}{\partial y} + \frac{1}{\mathrm{Re}}\left(\frac{\partial^2 v}{\partial^2 x} + \frac{\partial^2 v}{\partial^2 y}\right) + Gr/\mathrm{Re}^2 .T \tag{5}$$

Energy equation:

$$\frac{\partial T}{\partial t} + u\frac{\partial T}{\partial x} + v\frac{\partial T}{\partial y} = \frac{1}{\mathrm{Re}.\Pr}\left(\frac{\partial^2 T}{\partial^2 x} + \frac{\partial^2 T}{\partial^2 y}\right) \tag{6}$$

III. NUMERICAL METHOD

The governing equations are solved by CBS finite element method. The CBS algorithm for the solution of the Navier–Stokes and energy equation equations can be summarized by the following steps[19]:

1.Solution of the momentum equation without the pressure term.
2.Calculation of the pressure using the Poisson equation.
3.Correction of velocities.
4.Calculation of energy equation or any other scalar equation.
By applying the CBS method, the governing equations become as follows:
Step1:

$$\Delta\tilde{u}^* = -M_u^{\ -1}\Delta t[(C_u\tilde{u} + k_\tau\tilde{u} - f) - \Delta t(k_u\tilde{u} + f_s)]^n \tag{7}$$

Step2:

$$\begin{aligned}&(M_p + \Delta t^2\theta_1\theta_2 H)\Delta\tilde{p}\\ &= \Delta t[(G\tilde{u}^n + \theta_1 G\Delta\tilde{u}^* - \Delta t\theta_1 H\tilde{p}^n - f_p]\end{aligned} \tag{8}$$

Step3:

$$\begin{aligned}&\Delta\tilde{u}^{**} = \Delta\tilde{u} - \Delta\tilde{u}^*\\ &= -M_u^{\ -1}\Delta t[G^T(\tilde{p}^n + \theta_2\Delta\tilde{p}) + \frac{\Delta t}{2}P\tilde{p}^n]\end{aligned} \tag{9}$$

Step4:

$$\begin{aligned}&\Delta\tilde{E} = -M^{-1}{}_E\Delta t[C_E\tilde{E} + C_p\tilde{p} + K_T\tilde{T} + f_p]\\ &-\Delta t(K_{ue}\tilde{E} + K_{up}\tilde{p} + f_{es})\end{aligned} \tag{10}$$

ISBN: 978-988-18210-7-2
ISSN: 2078-0958 (Print); ISSN: 2078-0966 (Online)

Where overline parameters represent the nodal quantities. In the above equations, $\Delta\tilde{u}^{*}$ and $\Delta\tilde{u}^{**}$ are intermediate velocities, C_u, G, H and k_τ are discrete convection, gradient, Laplacian and viscous operators and M_u is the mass matrix and also θ_1 is the coefficient of stability parameter and θ_2 is a coefficient for switching between explicit $\theta_2 = 0$ and implicit ($0 < \theta_2 < 1$) scheme of solving the equations. In addition we have the following relation between the remaining coefficient matrices:

$$C_p = C_E = C_u,\ K_T = H = \frac{1}{\Pr} K_\tau,\ K_{up} = K_{ue} = K_u,$$

$$M_p = \frac{1}{\beta^2} M_u,\ M_E = M_u \tag{11}$$

The terms, f_s, K_u , P, K_{ue} and K_{up} are due to discretization along the characteristics and f, f_p and f_e contain the boundary conditions. The term f_{es} contains source terms.

The overlined parameters represent the nodal quantities. The non-real time step, t, (pseudo_time step) accelerates solution to steady state as fast as possible. The pseudo time step is locally calculated and subjected to stability condition.

$$\Delta t = \frac{h}{|u| + \beta} \tag{12}$$

Where h is the element size, β is the artificial compressibility parameter [17] and $|u|$ is the velocity.

IV. RESULT AND DISCUSSION

The main parameters of Rayleigh, Prandtl and Reynolds numbers on variations of mean Nusselt numbers of left, right and bottom and thermal and flow fields are examined. The local Nusselt number is calculated by the following equation:

$$Nu = -\frac{\partial T}{\partial n} \tag{13}$$

Where n denotes the normal direction on a plane. The dimensionless stream function ψ is defined as:

$$u = \frac{\partial \psi}{\partial y}, v = -\frac{\partial \psi}{\partial x} \tag{14}$$

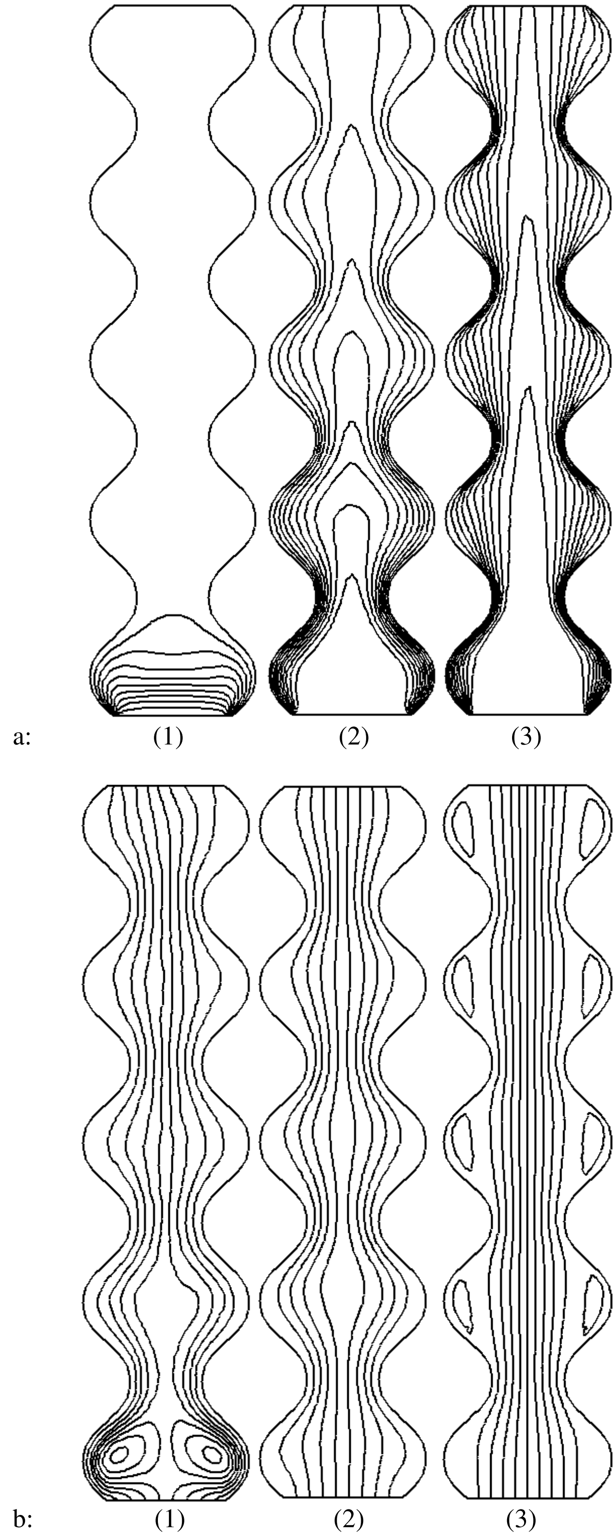

Fig. 2 Isothermal lines(a) and stream functions(b) at $Gr=10^5$, Pr=0.7 for different values of Reynolds number; (1).Re=10, (2).Re=100, (3).Re=500

In this study an unstructured linear triangular mesh corresponding 1300 nodes is utilized for all cases. Numerical solutions are obtained for various values of $Gr=10^4$–10^6, Pr=0.01–10 and Re=10–500.

ISBN: 978-988-18210-7-2
ISSN: 2078-0958 (Print); ISSN: 2078-0966 (Online)

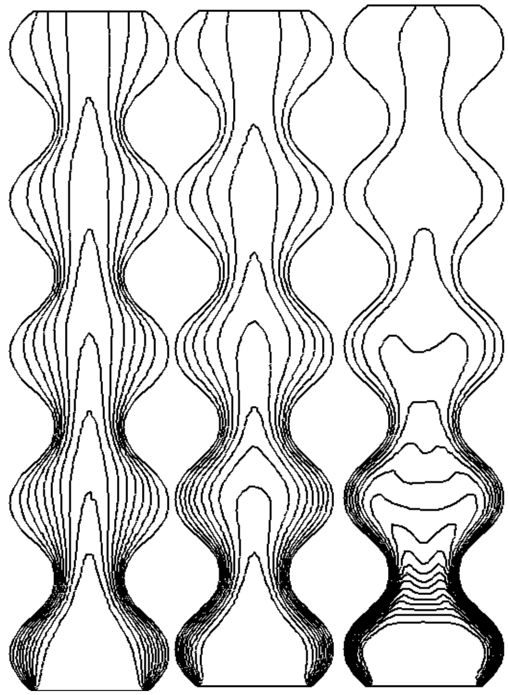

a: (1) (2) (3)

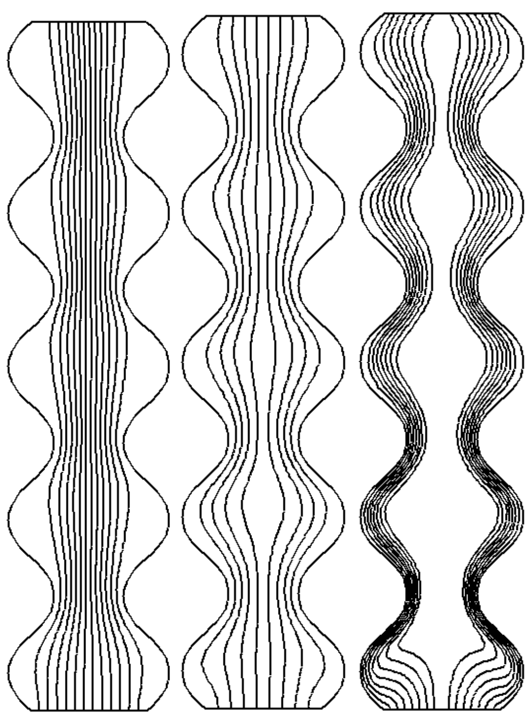

b: (1) (2) (3)

Fig. 3 Isothermal lines(a) and stream functions(b) at $Re=10^2$, $Pr=0.7$ for different values of Grashof number; (1),$Gr=10^4$, (2).$Gr=10^5$, (3).$Gr=10^6$

Effect of Reynolds number:

Fig.2 shows the isothermal lines and stream functions at $Gr=10^5$ and $Pr=0.7$ for different values of Reynolds number. For Re=10, two vertices produce due to uniform velocity of fluid at the inlet of the channel. Also plots for stream functions show that increment of Reynolds number results in production of small vertices at valleys. For Re=10 the temperature of cold entering fluid immediately reaches to T_h due to low velocity and momentum. With increasing Reynolds number the isotherms spreads all over the channel. It is also apparent that the compression of isotherms is increase due to curvature of side walls.

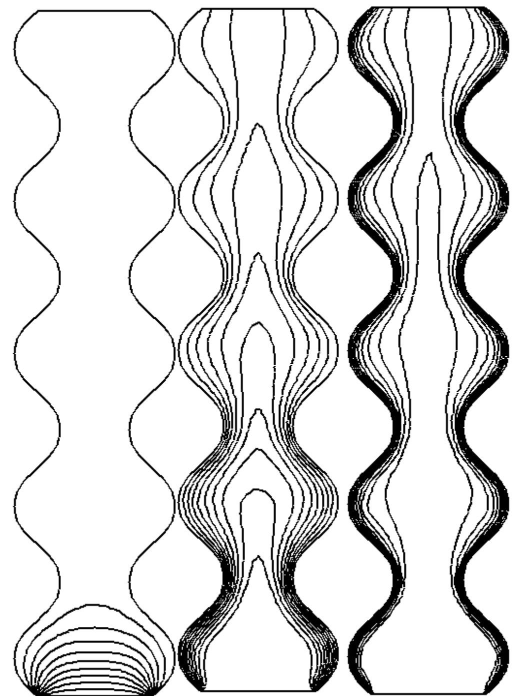

a: (1) (2) (3)

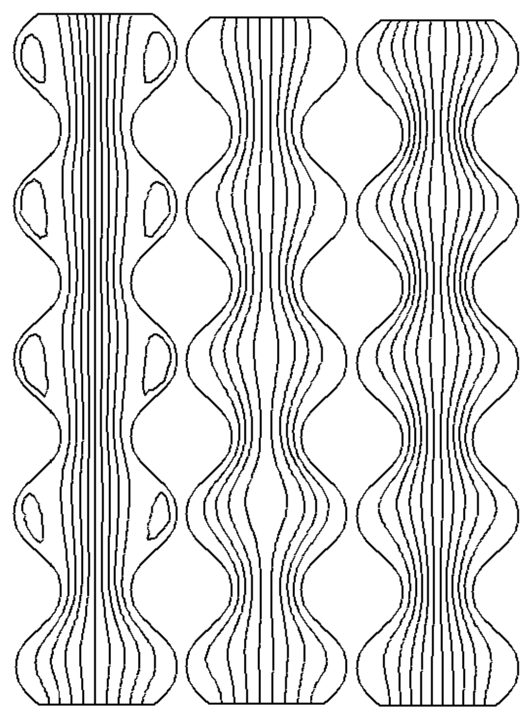

b: (1) (2) (3)

Fig. 4 Isothermal lines(a) and stream functions(b) at $Re=10^2$, $Gr=10^5$ for different values of Prantdl number; (1).$Pr=0.01$, (2).$Pr=0.7$, (3).$Pr=10$

ISBN: 978-988-18210-7-2
ISSN: 2078-0958 (Print); ISSN: 2078-0966 (Online)

Effect of Grashof number:

Fig.3 shows the isothermal lines and streamlines at Re=100 and Pr=0.7 for different values of Grashof number. With increment of Grashof number effect of buoyancy forces increases and excels the effect of forced convection which leads to decrement of peaks of isothermal lines at the middle of the channel. Increment of Grashof number also results in compression of isotherms at the inlet of the channel. Also at higher values of Grashof number the temperature of cold entering fluids will reach to T_h sooner than that of lower Grashof number. Stream functions for at higher values of Grashof number become more condense at the regions near the side walls due to stronger convection effects at the middle of the channel.

Effect of Prantdl number:

Fig.4 shows the isothermal lines and streamlines at Re=100 and Gr=10^5 for different values of prantdl number. At low values of Prantdl number, the temperature of the fluid rapidly reaches to the temperature of hot walls due to large value of thermal diffusivity. With increasing Prantdl number, increment of temperature of fluid will happen slowly, as a result the isotherms are more compressed along the channel near the hot walls. At Pr=0.01, a circulation will be produce at the valleys of the hot walls. With increment of Prantdl number theses vertices will disappear gradually.

Local Nusselt number:

Fig.5 shows the variations of local Nusselt number along the hot wall for different values of Grashof number for Re=10^2 and Pr=0.7. At the inlet of the channel the local Nusselt number is very large due to minimum thickness of boundary layer. With increasing y, the local Nusselt number will decrease due to decrement of temperature difference and

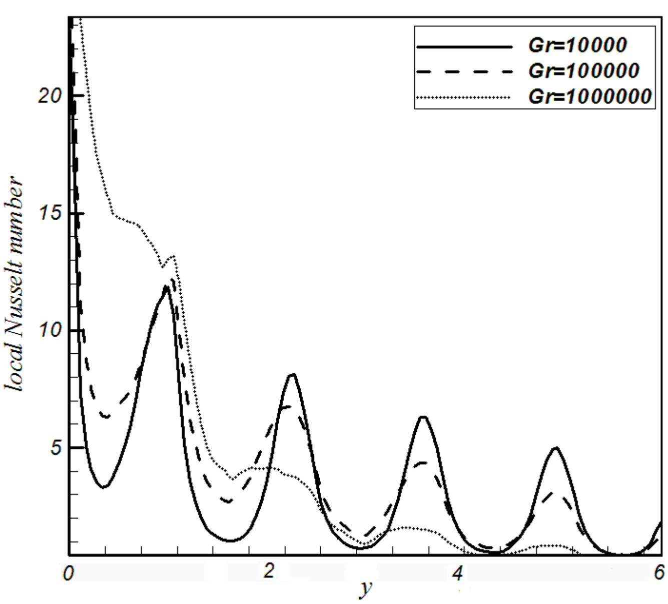

Fig. 5. Variations of local Nusselt number along the wavy wall of the channel for different values of Grashof number; Re=10^2, Pr=0.7.

increment of thickness of boundary layer, this trend will occurs more rapid with increment of Grashof number. Local Nusselt number will become relative maximum at the peaks of hot walls due to curvature of walls which results in increment of compression of isotherms.

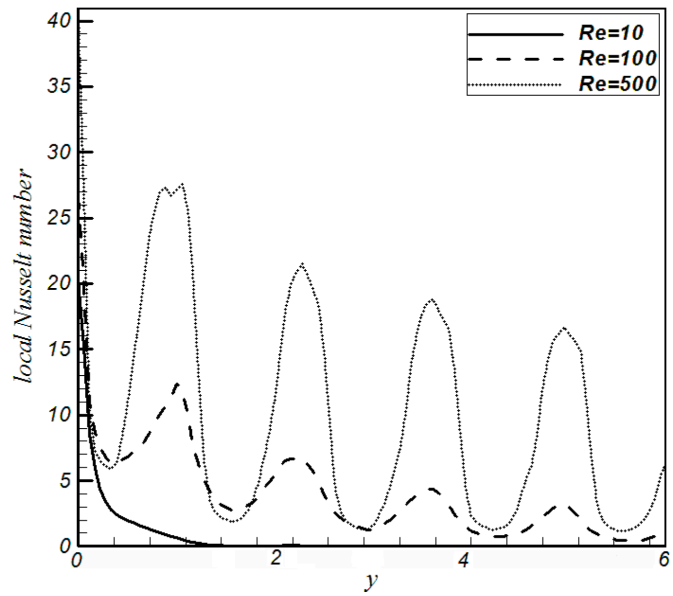

Fig. 6. Variations of local Nusselt number along the wavy wall of the channel for different values of Reynolds number; Gr=10^5, Pr=0.7.

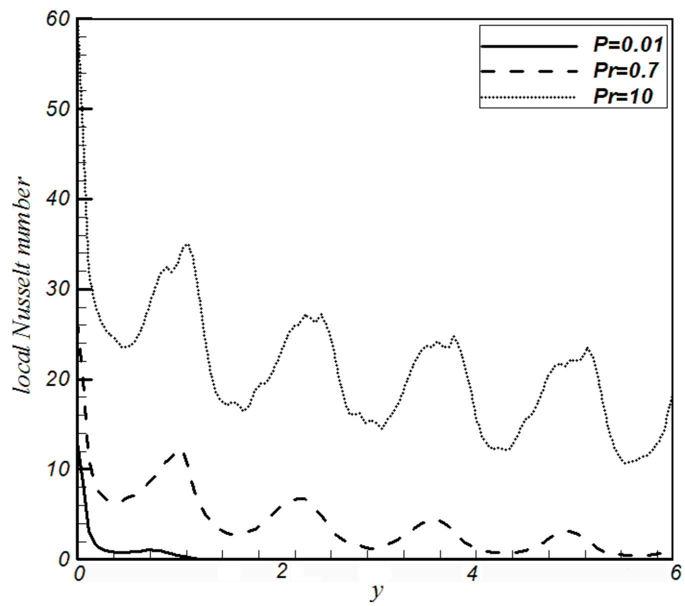

Fig. 7. Variations of local Nusselt number along the wavy wall of the channel for different values of Prantdl number; Re=10^2, Gr=10^5.

Fig.6 shows the plots for different values of Reynolds number for Gr=10^5 and Pr=0.7. At Re=10 the temperature of the fluid reaches to T_h rapidly, therefore the local Nusselt number become zero. Increment of values of Reynolds number will results in increasing of local Nusselt number. Similar to figure 5 the variations of local Nusselt number has relative maximum due to curvature of hot walls. Also with increasing y, the local Nusselt number will decrease due to decrement of temperature difference and increment of thickness of boundary layer.

ISBN: 978-988-18210-7-2
ISSN: 2078-0958 (Print); ISSN: 2078-0966 (Online)

Fig.7 shows the variations of local Nusselt number along the wavy wall of channel for different values of Prantdl number for Gr=10^5 and Re=10^2. For Pr=0.7 local Nusselt number rapidly become zero because the temperature of the fluid reaches the temperature of hot walls. With increasing the values of Prantdl number local Nusselt number of hot wall will increase due to enhanced thermal mixing. Similar to the other plots the local Nusselt number will decrease with increasing y through the channel due to decreasing the temperature difference.

V. Conclusion

In this work, mixed convection heat transfer through a wavy vertical channel has been investigated numerically by Galerkin finite element method based on the characteristic based split (CBS) algorithm. The effects of parameters such as Grashof number, Reynolds number and Prandtl number on flow and thermal fields through the channel. Results showed that with increasing Reynolds number and decreasing Prantdl number a secondary flow is produced at the valleys of hot walls. At higher values of Reynolds and Prantdl numbers the temperature of the fluid reaches to the value T_h later. Local Nusselt number of hot walls will decrease gradually through the channel and has relative maximum value at the peak of hot wavy wall. Also increasing the values of Reynolds and Prantdl number result in increasing the local Nusselt number of hot wall.

Acknowledgement

The authors are pleased to acknowledge the support of this study by University of Tehran, Tehran, Iran.
Authors also acknowledge help of Miss Moayedi for her valuable suggestions.

References

[1]J.-H. Jang, W.-M. Yan, Mixed convection heat and mass transfer along a vertical wavy surface, Int. J. Heat Mass Transfer 47 (2004) 419–428.

[2]P.K. Das, S. Mahmud, Numerical investigation of natural convection inside a wavy enclosure, Int. J. Therm. Sci. 42 (2003) 397–406.

[3]C.P. Chiu, H.M. Chou, Transient analysis of natural convection along a vertical wavy surface in micro polar fluids, Int. J. Eng. Sci. 32 (1994) 1933.

[4]D.A.S. Rees, I. Pop, A note on free convection along a vertical wavy surface in a porous medium, ASME J. Heat Transfer 116 (1994) 505–508.

[5] D.A.S. Rees, I. Pop, Free convection induced by a vertical wavy surface with uniform heat flux in a porous medium, ASME J. Heat Transfer 117 (1995) 547–550.

[6] Y.T. Yang, C.K. Chen, M.T. Lin, Natural convection of non-newtonian fluids along a wavy vertical plate including the magnetic field effect, Int. J. Heat Mass Transfer 39 (1996) 2831–2842.

[7] L.S. Yao, Natural convection along a vertical complex wavy surface, Int. J. Heat Mass Transfer 49 (2005) 281–286.

[8] M. Ashjaee, M. Amiri, J. Rostami, A correlation for free convection heat transfer from vertical wavy surfaces, Heat Mass Transfer 44 (2007) 101111.

[9]L.S. Yao, Natural convection along a wavy surface, ASME J. Heat Transfer 105 (1983) 465–468.

[10]L.S. Yao, A note on Prandtl_s transposition theorem, ASME J. Heat Transfer 110 (1988) 503–507.

[11] S.G. Moulic, L.S. Yao, Mixed convection along a wavy surface, ASME J. Heat Transfer 111 (1989) 974–979.

[12] C.P. Chiu, H.M. Chou, Transient analysis of natural convection along a vertical wavy surface in micropolar fluids, Int. J. Eng. Sci. 32 (1994) 1933.1082 J.-H. Jang et al. / International Journal of Heat andMass Transfer 46 (2003) 1075–1083

[13] C.K. Chen, C.C. Wang, Transient analysis of force convection along a wavy surface in micropolar fluids, AIAA J. Thermophys. Heat Transfer 14 (2000) 340–347.

[14] C.C. Wang, C.K. Chen, Transient force and free convection along a vertical wavy surface in micropolar fluids, Int. J. Heat Mass Transfer 44 (2001) 3241–3251.

[15] C.Y. Cheng, Natural convection heat and Mass transfer near a wavy cone with constant wall temperature and concentration in a porous medium, Mech. Res. Commun.27 (2000) 613–620.

[16] C.Y. Cheng, Natural convection heat and mass transfer near a vertical wavy surface with constant wall temperature and concentration in a porous medium, Int. Commun. Heat Mass Transfer 27 (2000) 1143–1154.

[17] P. Nithiarasu , C.-B. Liu. An artificial compressibility based characteristic based split (CBS) scheme for steady and unsteady turbulent incompressible flows Comput. Methods Appl. Mech. Engrg. 195 (2006) 2961–2982.